

Minimal Detectable Signal during Current Measurement in a CISPR 25 Set-Up

Zongyi Chen, Jin Jia, Stephan Frei

On-board System Lab
TU Dortmund University
Dortmund, Germany
zongyi.chen@tu-dortmund.de

Syed Huq, David Pommerenke

EMC Laboratory
Missouri University S&T
Rolla, MO, USA
shwdf@mst.edu

Abstract—This paper investigates instrumentation effects that may limit the usefulness of pre-compliance bench-top test methods for e.g. CISPR 25 radiated field measurements. Here the radiated fields are dominated by common-mode currents along the test cable bundle especially when the frequency is below several hundred MHz. From a known current distribution, fields can be computed. The currents can be measured using current probes with measurement instruments like oscilloscopes or spectrum analyzers (SAs). However, because of the low CISPR limits, very small currents (amplitude and phase) need to be measured. In this paper, as first step, the current values that lead to emissions at the CISPR limit are determined using method of moment (MoM) simulations. For analyzing the practical sensitivity of typical current measurement instruments, the noise figures of oscilloscopes and SAs are approximately measured and the compete measurement system is optimized with respect to probe selection and pre-amplification. It is shown that oscilloscopes and SAs achieve similar sensitivities, and both having noise figures in the range of 15–25 dB without pre-amplification. By setting corresponding fast Fourier transformation (FFT) parameters it is possible to obtain the same bandwidths in an oscilloscope as in a SA for the bandwidths typically used in electromagnetic interference (EMI) measurements. Further, oscilloscope-based phase measurement is explained. The noise induced errors are shown for the magnitude and phase indicating a lower minimal detectable signal of about -25 dB μ A for less than 15° phase error.

Keywords— CISPR 25; current probe; oscilloscopes; spectrum analyzers (SAs); noise figure; spurious

I. INTRODUCTION

In a typical CISPR 25 field measurement set-up [1], antennas are used to measure the field strength while the equipment under test (EUT) is mounted on a metallic table. A variety of papers have analyzed pre-compliance bench-top methods. In [2-4] a current probe is used to measure the current distribution along the cable bundle. An equivalent multi-dipole radiation model is created from the measured currents and can be used for emission prediction. An example is shown in [2], where an oscilloscope is used in conjunction with a reference probe, in this case current magnitude and phase information can be directly obtained through Fast Fourier Transformation (FFT). If a SA is used, only the current magnitude can be directly obtained. The phase information needs to be retrieved through optimization algorithms based on transmission line theory or through methods outlined e.g. in [5-6].

However, most papers mainly focus on validation of the proposed alternative methods by comparing predicted electric field against results from a standard antenna measurement method; they barely discuss the detectable current limits in measurement systems.

The limit levels of the electric field also restrict the current on the cable bundle. As specified in [1], for Class 5 of the absorber lined shielding enclosure (ALSE) method, when average detector is used, the limit level for the electric field at 100 MHz and at 300 MHz is 18 dB μ V/m. For observing the current magnitude that radiates a signal just at the limit level, a simulation set-up was created. As shown in Fig. 1, the set-up contains a source V_0 having a source impedance of $Z_{\text{Source}} = 50 \Omega$, a transmission line (a simplified cable bundle) of 1.5 m length 5 cm above metallic table, and a termination $Z_{\text{Load}} = 50 \Omega$. The characteristic impedance of the cable Z_C is 276 Ω . This is modelled to determine the fields at an assumed antenna reference point (1 m distance from cable center). As illustrated in [1], the metallic table is at a height of 90 cm above the chamber floor, which is not shown in the figure.

Simulated current magnitude distributions which cause the calculated electric fields in vertical polarization (Fig. 2 a) and in horizontal polarization (Fig. 2 b) equal to the limit level are shown respectively. It shows the current needed to cause a field at the limit level can be very low. For example, the maximal current on the transmission line at 300 MHz is less than -5 dB μ A in vertical polarization (Fig. 2 a). Measuring such low level currents require a highly sensitive measurement system.

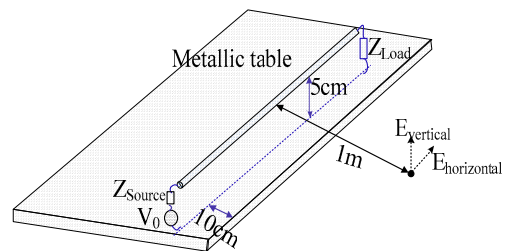


Fig. 1 Sketch of CISPR 25 ALSE test set-up

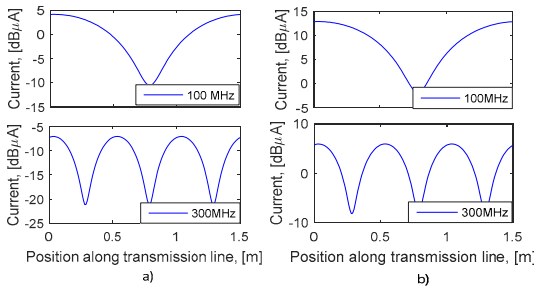


Fig. 2 Currents along the transmission line. a) Shows currents cause the calculated E_{vertical} at antenna reference point that equal the field limit given in regulation, b) Shows currents cause the calculated $E_{\text{horizontal}}$ at antenna reference point that equal the field limit given in regulation

This paper shows that an oscilloscope and a SA have similar sensitivity limits, even both are used without a pre-amplifier. If a well-chosen pre-amplification is used, both types of instrument set-ups show the same noise floor, as the noise floor is only defined by the noise figure of the pre-amplification. However, the oscilloscope's usability may be limited at certain frequencies due to spurious signals.

II. NOISE LIMIT

A rough estimation of noise figure is given by:

$$NF = [P_{\text{NOUT}} - (-174 + 10\log(RBW) + G)] \quad (1)[7]$$

where NF is the noise figure in dB. P_{NOUT} is the measured total output noise power in dBm. -174 is noise density in dBm/Hz, calculated at room temperature (290 K). RBW is resolution bandwidth in Hz. G is system gain in dB (this correction is only needed if a pre-amplifier is used).

A. Noise Figure Estimation of Oscilloscopes

Noise performance of different oscilloscopes were evaluated using equation (1). 8-bit oscilloscopes from different vendors (such as LeCroy, Agilent, Tektronix) were compared. For noise figure estimation, the smallest vertical scale (highest vertical sensitivity) and the fastest sampling rate was used. The noise figure was estimated using two methods:

1) Broadband

Here, the $V_{\text{rms(AC)}}$ noise floor is displayed when the smallest V/div setting is used. For example, an oscilloscope (sampling rate 20 Gs/s) showed $V_{\text{rms(AC)}} (= 259 \mu\text{V})$. Using the nominal bandwidth of the oscilloscope (4 GHz) and assuming that the noise is uniformly distributed over all frequencies, and that the spurious signals do not significantly contribute to the noise amplitude, then a noise figure of 19 dB is estimated. Table 1 shows the estimated noise figures of oscilloscopes from LeCroy, Agilent and Tektronix.

TABLE I. NOISE FIGURE (BROADBAND) ESTIMATION

Oscilloscopes	LeCroy Wavemaster 8620A	Tektronix TDS7404	Agilent infiniium DSO9404A
Nominal bandwidth	6 GHz	4 GHz	4 GHz
Vertical div	2 mV/div	2 mV/div	1 mV/div
Sampling rate	20 GS/s	20 GS/s	20 GS/s
Data points	4M	2M	200k

Oscilloscopes	LeCroy Wavemaster 8620A	Tektronix TDS7404	Agilent infiniium DSO9404A
Nominal bandwidth	6 GHz	4 GHz	4 GHz
Vsdev(rms)	444 uV	300 uV	446 uV
NF	24	19	24

2) Narrowband

The noise figure can also be estimated based on the noise floor shown within the FFT. For example, if the FFT center frequency is set to 100 MHz (one needs to ensure that there are no spurious signals at this frequency) and a FFT bandwidth of 10 kHz is selected (using flat-top windowing function [8]) the averaged magnitude may show a value of -115 dBm. Using the bandwidth and the average noise floor, a noise figure of 19 dB is estimated.

Typically oscilloscopes we measured showed noise figures in the range of 15–25 dB.

B. Noise Figure Estimation of SAs

The noise level of a SA is commonly referred to as displayed average noise level (DANL). Equation (1) can also be used to estimate the noise figure of a SA. Here, the equivalent noise bandwidth should be used instead of the RBW; however, the differences between the noise bandwidth and the RBW are small. Fig. 3 presents a screenshot with DANL of -115dBm measured in a 10 kHz RBW and with 0 dB attenuation, NF in this case is 19 dB. Additional corrections can be introduced by averaging in linear scale or by directly reading the noise density using a noise cursor. However, these corrections are only a few dB and not important for noise figures between 15 and 25 dB without pre-amplification.

C. Noise Figure Comparison of Oscilloscope and SA with/without Preamplifier

For comparing the sensitivity limits between a SA and an oscilloscope, the same RBW was used. The RBW of the oscilloscope is realized by the FFT and the windowing function. To improve the noise figure of the system, a 50 dB gain, 3 dB noise figure amplifiers was used. Thus, the overall system noise figure is close to 3 dB.

D. Spurious-Free Dynamic Range (SFDR)

The spurious-free dynamic range (SFDR) is defined as the ratio of a signal that fully uses the A/D converter to the first largest spurious signal. To measure SFDR, a clean sine wave generator (harmonics are suppressed by an added low pass) is applied to the oscilloscope. The amplitude of the sine wave is set to use full range of the A/D converter. The FFT of the signal is taken and the ratio of the intended signal to the strongest spurious signal is taken as the SFDR. Measuring six oscilloscopes (all 20 GS/s) showed SFDR values between 40 and 55 dB. As an example for measuring SFDR, Fig. 4 illustrates when spurious-free signal fundamental frequency is applied and compared with the next largest spurious spectrum. The oscilloscope under test has about 40 dB SFDR. A low spurious level is important as it may not be possible to measure the current on the cable harness at a frequency at which the oscilloscope has a spurious signal.

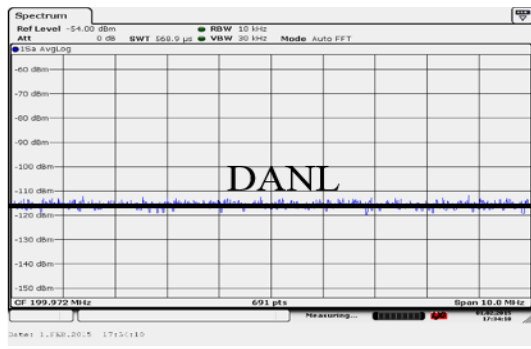


Fig. 3 An illustration of DANL determination

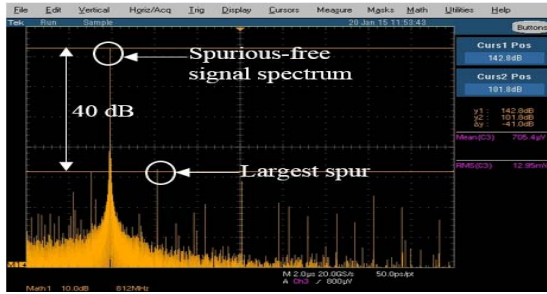


Fig. 4 An illustration of SFDR determination

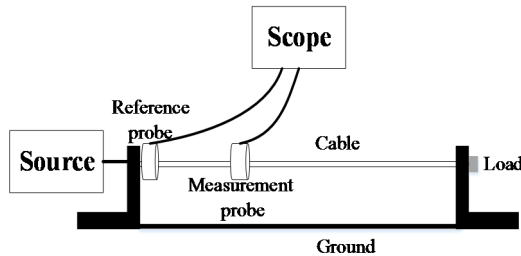


Fig. 5 Phase-resolving measurement set-up using oscilloscope

III. PHASE-RESOLVED CURRENT MEASUREMENT

An oscilloscope is used for a phase-resolved current measurement for the CISPR 25 set-up (shown in Fig. 5). The measurement is based on the segmentation method [2-4].

A. Phase and Magnitude Measured with Oscilloscope

Current probes with a transfer impedance of $0 \text{ dB}\Omega$ and a $15 \text{ dB}\Omega$ were used. To determine the sensitivity, tests were conducted with and without pre-amplification at different signal levels. The signal source frequency was fixed at 199.97 MHz; choosing this frequency was to avoid a spurious signal at 200 MHz of the oscilloscope (Agilent Infinium DSO9404A). Fig. 6 shows the phase and magnitude distribution (displayed as mean value) of the current along the transmission line using the $0 \text{ dB}\Omega$ transfer impedance current probe for source powers of -30 dBm and -40 dBm . The minimum of the current is a result of the 231Ω transmission line being terminated by 50Ω . The data shows that this set-up can resolve currents of about $20 \text{ dB}\mu\text{A}$ within 10° phase error.

Fig. 7 shows results of the optimized system including a $15 \text{ dB}\Omega$ transfer impedance current probe and 50 dB amplification (3 dB noise figure). The data presented indicates that a stable current magnitude distribution can be captured when the source power is decreased to -80 dBm . It should be noted that the value of source power also depends on the termination impedances. Under these circumstances the phase deviation is less than 15° and magnitude deviation is within 2 dB . In Fig. 7, the data shows the practical limit of the measurement process for the optimized set-up in which pre-amplifiers are used. If the source was set to -80 dBm (black curves) the current minima is at about $-25 \text{ dB}\mu\text{A}$. The standard deviation (SD) of magnitude is about 2 dB at the worst spot and the SD for the phase measurement is about 15° . However, if the signal generator is set to -90 dBm , the current drops to about $-35 \text{ dB}\mu\text{A}$. The SD of the current magnitude surpasses 5 dB and the phase practically cannot be resolved at the location of the current minimum. Thus, currents of $-25 \text{ dB}\mu\text{A}$ can be taken as the minimal detectable value for the optimized system.

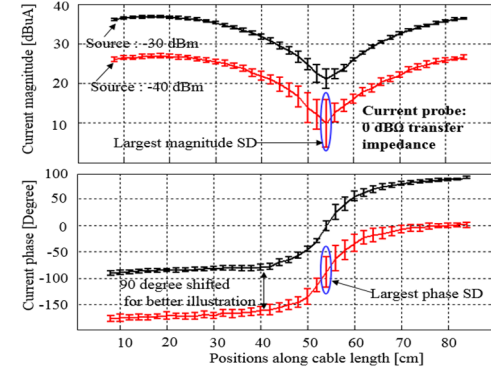


Fig. 6 Current magnitude (upper) and phase (lower) measurements (at 9 kHz RBW) using a current probe of $0 \text{ dB}\Omega$ transfer impedance without pre-amplifier. The vertical bar indicates the standard deviation

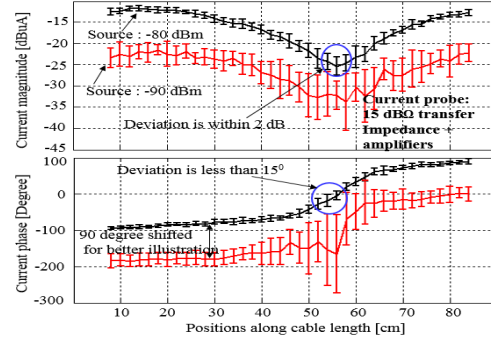


Fig. 7 Current magnitude (upper) and phase (lower) measurements (at 9 kHz RBW) using a current probe of $15 \text{ dB}\Omega$ transfer impedance with pre-amplifier. The vertical bar indicates the standard deviation.

B. Comparison of Current Magnitude Measured with Oscilloscope and SA

As shown in Fig. 8, the source was set to -50 dBm (upper) and to -90 dBm (lower). The figures indicate that the magnitude readings of the SA and oscilloscope are within 1 dB . Occasionally, larger deviations were observed. However, from an EMC point of view the differences are not significant. The

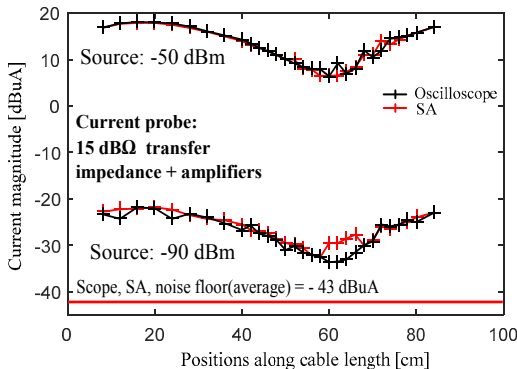


Fig. 8 Current amplitudes measured (at 9 kHz RBW) using oscilloscope and SA with 15 $\text{d}\Omega$ transfer impedance current probe with pre-amplifiers

averaged noise floor for the optimized set-up is at about -43 $\text{d}\mu\text{A}$ (evaluated using equation (1)). The noise floor is identical as pre-amplification is used and both instruments use the same bandwidth (defined by the FFT parameters for the oscilloscope and the RBW for the SA).

IV. CONCLUSION

This paper investigated instrumentation effects that may limit the usefulness of pre-compliance bench-top test methods. It discusses the achievable sensitivities of CM-current measurements and concludes that both oscilloscopes and SAs can achieve the needed sensitivity if sensitive current clamps and low noise pre-amplifiers are used. It further shows that the noise figures of SAs and oscilloscopes are around 15-25 dB if no pre-amplifier is used. Without pre-amplifier and a probe having a 0 $\text{d}\Omega$ transfer impedance, both the oscilloscope and the SA can resolve signals of 10 $\text{d}\mu\text{A}$ at about 9 kHz RBW. The most sensitive case investigated was the combination of a 15 $\text{d}\Omega$ transfer impedance probe with 3 dB NF pre-amplifiers. In this case, a signal of -33 $\text{d}\mu\text{A}$ will be detected at about 10 dB above the average noise floor. However, if an oscilloscope is used the spurious signals of the oscilloscope itself may limit the lowest detectable signal at the specific frequencies of the spurious signals.

REFERENCES

- [1] CISPR 25 Ed.4, "Vehicles, boats and internal combustion engines-Radio disturbance characteristics – Limits and methods of measurements for the protection of on-board receivers", 2015.
- [2] J. Jia, D. Rinas, and S. Frei, "An alternative method for measurement of radiated emissions according to CISPR 25," *IEEE Int. Symp. Electromagn. Compat.*, pp. 304-309, September 2013.
- [3] W. Smith and R. Frazier, "Prediction of anechoic chamber radiated emissions measurements through use of empirically-derived transfer functions and laboratory common-mode current measurements," in *Proc. IEEE Int. Symp. Electromagn. Compat.*, vol. 1, pp. 387-392. 1998.
- [4] D. Schneider, M. Bottcher, B. Schoch, S. Hurst, "Transfer functions and current distribution algorithm for the calculation of radiated emissions of automotive components," *IEEE Int. Symp. Electromagn. Compat.*, pp. 443-448, September 2013.
- [5] Z. Chen, S. Marathe, H. Kajbaf, S. Frei, D. Pommerenke, "Broadband phase resolving spectrum analyzer measurement for EMI scanning application", *IEEE Int. Symp. Electromagn. Compat.*, pp. 1278-1283, August 2015.
- [6] A. Ramanujan, F. Lafon, P. Lopez, "Radiated emissions modelling from near-field data - toward international standards", *IEEE Int. Electromagn. Compat.*, AP EMC, pp. 90-93. 2015.
- [7] R. Adler, M. Lebenbaum, A. H. Haus, W. Mumford, R. Engelbrecht, and S. Harrison, "Description of noise performance of amplifiers and receiving systems," *Proc. IRE*, vol. 51, pp. 436-442, March 1963.
- [8] Gade, Svend, and Henrik Herlufsen. "Use of Weighting Functions in DFT/FFT Analysis (Part I)." *Windows to FFT Analysis (Part I): Briel & Kjaer Technical Review*, No. 3, 1987, pp. 1-28.